The 7-days-exposure to gamma-hexachlorocyclohexane causes resistance to insulin in differentiated mature 3T3-L1 adipocytes

(7 日間のガンマ型シクロクロロヘキサンへの暴露は成熟型 3T3-L1 脂肪細胞にインスリン抵抗性を惹起する)

旭川医科大学大学院医学系研究科博士課程医学専攻

阿里木　阿米熱

(小笠原　準悦,　白土　健,　吉田　貴彦)

原著論文

7 日間のガンマ型シクロクロロヘキサンへの暴露は成熟型 3T3-L1 脂肪細胞にインスリン抵抗性を惹起する

アリム　アミラ [1)]，小笠原準悦 [1)]，白土　健 [2)]，吉田貴彦 [1)]

1)　旭川医科大学医学部社会医学講座衛生学・健康科学分野
2)　杏林大学医学部衛生学公衆衛生学講座

略題：シクロクロロヘキサンが誘導する成熟脂肪細胞のインスリン抵抗性

キーワード：ガンマ型ヘキサクロロシクロヘキサン，成熟型白色脂肪細胞，インスリン抵抗性，グルコース輸送単体 4

責任著者：吉田貴彦，旭川医科大学医学部社会医学講座衛生学・健康科学分野
住所：078-8510　旭川市緑が丘東 2 条 1 丁目 1-1
電話番号：0166-68-2402
Fax 番号：0166-68-2409

The 7-days-exposure to gamma-hexachlorocyclohexane causes resistance to insulin in differentiated mature 3T3-L1 adipocytes

Amire Alimu[1)], Junetsu Ogasawara[1)], Ken Shirato[2)], Takahiko Yoshida[1)]

1) Division in Hygiene and Health Science, Department of Social Medicine, Asahikawa Medical University, School of Medicine
2) Department of Molecular Predictive Medicine and Sport Science, Kyorin University, School of Medicine

To whom correspondence should be addressed: Takahiko Yoshida, M.D., Ph.D
Division of Hygiene and Health Science, Department of Social Medicine, Asahikawa Medical University, School of Medicine, 2-1-1-1 Midorigaoka Higashi, Asahikawa, Hokkaido 078-8510, Japan
E-mail address: tyoshida@asahikawa-med.ac.jp
Tel: +81-166-68-2400
Fax: +81-166-85-2409

抄録

本研究の目的は、有機塩素系農薬であるガンマ型ヘキサクロロシクロヘキサン（γ-HCH）が成熟型脂肪細胞へおよぼす影響について検討することである。成熟型に分化した 3T3-L1 脂肪細胞をγ-HCH の存在下と非存在下で 37℃、5%濃度の二酸化炭素の環境において 7 日間培養した。培養終了後に細胞の生存率、インスリン添加によるグルコースの取り込み能、細胞内活性酸素の発現量を蛍光アッセイ法にて測定した。mRNA とタンパク質の発現は、それぞれ定量 PCR 法とイミュノブロッティング法にて測定した。γ-HCH の添加は、非添加と比較してインスリン刺激による細胞へのグルコースの取り込みを有意に低下させ、細胞内の活性酸素量を有意に増加させた。この状況下では、細胞膜上における GLUT4 タンパク質の発現が有意に低下した。γ-HCH の添加によって、活性酸素の発現マーカーである分子群の mRNA 発現と JNK タンパク質のリン酸化も有意に増加した。さらに、γ-HCH の添加はインスリン刺激による糖取り込みを抑制する IRS-1 タンパク質の 307 番目にあるセリン残基のリン酸化を有意に増加させ、その下流に存在する AKT2 タンパク質と AS160 タンパク質のリン酸化を有意に抑制した。一連の結果より、γ-HCH の添加は細胞内の活性酸素量を増加させ、それに伴い活性化された JNK タンパク質が IRS-1 の 307 にあるセリン残基のリン酸化を増加させることによって AKT2 タンパク質と AS160 タンパク質の活性が有意に低下し、これに伴い GLUT4 タンパク質の細胞膜への移行が阻害されることによってインスリン刺激によるグルコースの取り込みが低下する、インスリン抵抗性が生じることが明らかとなった。

Abstract

The object of this study is to elucidate the effect of gamma-hexachlorocyclohexane (γ-HCH), an organochloride pesticide, on glucose uptake in fully differentiated mature 3T3-L1 adipocytes. Differentiated mature adipocytes were treated with or without γ-HCH for 7 days at 37°C in a 5% CO_2 incubator. After that, both cell viability and glucose uptake were measured by colorimetric assay, and generation of intracellular reactive oxygen species (ROS) were measured by fluorescence assay. Levels of mRNA and protein were analyzed using real-time polymerase chain reaction and immunoblotting, respectively. Treatment with sub-toxic doses of γ-HCH decreased insulin-stimulated glucose uptake, enhanced the production of ROS, and upregulated glucose transporter 4 (GLUT4) while reducing its translocation to the plasma membrane. Treatment with γ-HCH also stimulated the expression of markers of ROS production and phosphorylation of c-Jun N-terminal kinase (JNK). Moreover, phosphorylation of serine-307 (Ser307) in insulin receptor substrate-1 (IRS-1), which has an inhibitory effect on insulin-mediated glucose uptake, was increased, whereas the phosphorylation of AKT2 and/or AKT substrate 160 (AS160) proteins decreased. These findings indicate that γ-HCH attenuated insulin-stimulated glucose uptake in mature 3T3-L1 adipocytes by reducing the translocation of GLUT4 protein to the plasma membrane via the phosphorylation of Ser307 in IRS-1 and ROS-stimulated activation of JNK.

Key words: Gamma-hexachlorocyclohexane, mature 3T3-L1 adipocyte, insulin resistance, glucose transporter 4

Introduction

The prevalence of type 2 diabetes mellitus (T2DM) has recently increased in developing countries.[1,2] In addition to obesity, it has been reported that the exposure to persistent organic compounds, most commonly pesticides, cause T2DM.[3-6] They also cause other metabolic diseases in humans[3-6] positively associated with T2DM and related metabolic conditions.[5,6] It has been suggested a correlation between the development of T2DM with chronic exposure to pesticides via direct oral intake and food chain.

Gamma-hexachlorocyclohexane (γ-HCH) is a common insecticide used in agriculture worldwide.[7] However, γ-HCH has toxic effects on humans, such as in the development of diseases of the central nervous system, blindness, mental confusion, convulsion, and dysarthria.[7] Therefore, γ-HCH has been banned in several developed countries and it has been included as a persistent organic pollutant in 2009 by the Stockholm Convention. Nevertheless, γ-HCH is popular in developing countries,[8] although this chemical directly or indirectly damages the ecosystem. The increase in occurrence of T2DM in developing countries[1,2] may be correlated with chronic exposure to γ-HCH. Indeed, it has been reported that γ-HCH is also associated with dyslipidemia[9] and accumulates in adipose tissue.[10,11]

Mature adipocytes constitute the principal part of adipose tissue. Therefore, it is hypothesized that γ-HCH affects adipocytes resulting in the occurrence of T2DM. However, little is known about the toxic effects of γ-HCH on the physiological responses in mature adipocytes. The NOEL (dose, no observable effect level) of γ-HCH is 600 mg/L in L6-derived myotubes.[12] This concentration corresponds to approximately 2 mM (MW: 290.83). Therefore, to determine the cytotoxic and sub-toxic dose of γ-HCH in mature 3T3-L1 adipocytes, cell viability should be examined at various concentrations of γ-HCH from low levels to 1000 μM.

It is also hypothesized that γ-HCH affects the many mechanisms related to the T2DM. Adipocyte uptakes glucose by insulin stimulation. If this mechanism was impaired, it would result in impaired glucose tolerance. The translocation of glucose transporter 4 (GLUT 4) protein from the cytosol to the plasma membrane plays a key role in insulin-stimulated glucose uptake in adipocytes.[13-15] Therefore, it is useful to determine the modification of GLUT4, by determination of the mRNA levels of GLUT4 and intracellular localization of GLUT4 protein for elucidation whether γ-HCH affects insulin-stimulated uptake via GLUT4. It is known that excessive intracellular ROS suppresses the translocation of GLUT4 protein in 3T3-L1 adipocytes.[16] Previous study demonstrated that chronic up-regulation of reactive oxygen species (ROS) induced by γ-HCH caused insulin resistance in 3T3-L1 preadipocytes.[16] Also, γ-HCH enhances intracellular ROS production in Ehrlich ascites tumor cells[17] and human lymphocytes.[18] To elucidate the mechanism related to glucose uptake in adipose cells resulting in insulin resistance in mature adipocytes, it is necessary to examine the modification of ROS production in adipocytes (intracellular ROS production) by γ-HCH.

Many ROS markers have been known such as cytochrome P450 1b1, haptoglobin, ceruloplasmin 350, and xanthine dehydrogenase. ROS markers are overexpressed upon the generation of intracellular ROS.[19] In addition, the levels of NADPH oxidase-4 (Nox-4) mRNA and nuclear factor erythroid 2-related factor 2 (Nrf2) have shown to be increased by intracellular ROS generation in 3T3-L1 adipocytes.[20,21] Therefore, it is useful to examine levels of these markers in adipose tissues exposed to γ-HCH by determination of mRNA expressions of them.

Excessive ROS stimulates the phosphorylation of c-Jun N-terminal kinase (JNK), thereby activating JNK in 3T3-L1 adipocytes.[22] The phosphorylation of IRS-1 at Ser307 is a target of JNK. Other targets of JNK are known, which are related to glucose uptake in adipocytes, such as phosphorylation of AS160, which participates in insulin-stimulated GLUT4 translocation downstream of AKT2,[23] and phosphorylation of AKT2, a key molecule in the activation of insulin-stimulated glucose uptake.[24] Previous study reported that the inactivation of IRS-1 upon phosphorylation at Ser307 and subsequent inhibition of insulin-related signal transduction.[25] It is useful to examine the expressions of these genes to elucidate the possible impaired mechanism of glucose uptake by γ-HCH whether or not γ-HCH affect the phosphorylation. It has shown that TNF-α triggers the activation of JNK, thereby impairing insulin action.[26] It is also useful to examine determine whether γ-HCH stimulates selection of TNF-α, or increases the mRNA expression of TNF-α.

The objective of this study is to elucidate the effects of γ-HCH on insulin resistance in mature

3T3-L1 adipocytes and the molecular mechanisms underlying possible γ-HCH-induced modification in signal transduction cascade of glucose uptake by insulin stimulation. For this objective, the effects on γ-HCH on the followings in the mature adipocytes were examined; the cytotoxic level of γ-HCH, insulin-stimulated glucose uptake, translocation event of GLUT 4 protein on the plasma membrane, ROS production, the activation of AKT2 and the phosphorylation of Ser307 in insulin receptor substrate-1 (IRS-1), and the mRNA expression and secretion of TNF-α.

Materials and Methods

Culturing 3T3-L1 preadipocyte to mature adipocytes and treatment of γ-HCH

3T3-L1preadipocytes were purchased from KAC Co. Ltd. (Kyoto, Japan). 3T3-L1 preadipocytes were seeded in a 25 cm^2 collagen 1-coated flask (Thermo Scientific, NY) and grown till confluence in 3T3-L1 preadipocyte medium (Zen-Bio, Inc., NC). The cells were maintained in the same medium for 2 days post-confluence at 37°C in a 5% CO_2 incubator. Cellular differentiation was induced by treatment with 3T3-L1 differentiation medium (Zen-Bio, Inc., NC) for 3 days. Cells were cultured for 4 more days in 3T3-L1 adipocyte medium (Zen-Bio, Inc., NC) to be differentiated mature adipocytes.

Subsequently, differentiated mature 3T3-L1 adipocytes were cultured in collagen 1-coated 24-well plates (Corning, Inc., ME) with (γ-HCH group) or without γ-HCH (control group) in 1 ml of medium per well for 7 days in incubator. The medium was changed every 2–3 days.

Cell viability of the mature adipocytes exposed to γ-HCH

Differentiated mature adipocytes were treated with 0μM, 25 μM, 50 μM, 100 μM, and 1000 μM γ-HCH for 7 days. At the end of cultivation, cell culture media were collected and cell viability was determined using the LDH cytotoxicity detection kit (Takara Bio, Inc., Shiga, Japan) according to the manufacturer's instructions. The subtoxic level was determined based on the results of cell viability. The subtoxic level would be the level in which there was no significant difference in the cell viability compared to the control and there were no big variances in the cell viability in the group. The concentration 50 μM of γ-HCH in the following experiments were the subtoxic level determined here.

To adjust the data determined by LDH amount, the remaining cells were harvested using a cell scraper and resuspended in a solution of protease inhibitor cocktail (Nacalai Tesuque, Kyoto, Japan) and phosphatase inhibitor (Nacalai Tesuque, Kyoto, Japan) including M-PER Mammalian protein extraction reagent (Thermo Scientific, NY). Data were calculated by dividing the total protein concentration of each well.

Insulin-stimulated glucose uptake

After 7 days of cultivation with or without γ-HCH, the culture medium was aspirated and cells were cultured in serum-free culture medium for 6 h in CO_2 incubator. After incubation, cells were washed three times with buffer A (Krebs Ringer Phosphate Hepes buffered with 1.2 mM KH_2PO_4, 1.2 mM $MgSO_4$, 1.3 mM $CaCl_2$, 118 mM NaCl, 5 mM KCl, 30 mM Hepes, pH 7.5). Buffer A containing 2% BSA (essential fatty acid free, Sigma Ca. No. A0281, Sigma Aldrich, MO). Ten μl of 100μM insulin was added to each well at the final concentration as 1 μM and the plates were incubated for 18 min in CO_2 incubator. Next, 2-deoxyglucose (Nacalai Tesuque, Kyoto, Japan) was added at the final concentration as 1 mM and incubated for 20 min in CO_2 incubator. The culture medium was removed and cells were washed three times with phosphate-buffered saline containing 200 μM phloretin (Sigma-Aldrich, MO), a glucose uptake inhibitor. The cells were harvested using a cell scraper in 10 mM Tris-HCl (pH 8.0). The cellular suspension was homogenized by 30 passages using a 5/8-inch 27-gauge needle attached to a syringe. The homogenate was heated at 80°C for 15 min and centrifuged at 15,000×g at 4°C for 20 min. The obtained supernatant was used as the sample for the analysis of glucose uptake. The amount of 2-deoxyglucose was determined using the commercially available 2-Deoxyglucose uptake measurement kit (Cosmo Bio Co., Ltd., Tokyo, Japan) according to the manufacturer's instructions.

Intracellular ROS levels

The cells were seeded and grown in collagen 1-coated 96-well plates and differentiated/treated with or without γ-HCH as described above. Intracellular ROS levels were measured using the ROS-Glo ™ H_2O_2 Assay kit (Promega, WI) and fluorescence microplate reader. After the measurement, cell numbers were counted in each well using the Cell Count Normalization Kit (Dojindo Laboratories, Kumamoto, Japan) according to the manufacturer's instructions.

Quantitative real-time polymerase chain reaction (PCR)

After 7 days treatment of 3T3-L1 cells with or without γ-HCH, total RNA in the cytoplasm was extracted for following experiment. The total RNA was extracted using TRI Reagent, Direct-zol ™ RNA Miniprep kit (Zymo Research, CA). Complementary DNA was synthesized using the Super Script® IV First-Strand cDNA synthesis reaction system using the Oligodt primer (Invitrogen) and RNase inhibitor (Toyobo, Tokyo, Japan). For real-time PCR, RNA was reverse transcribed using the PowerUp™SYBER Green Master Mix (Thermo Fisher Scientific, CA) and amplified using the Applied Biosystems StepOne®Real-Time PCR system (Waltham, MA). The amplification protocol included a hold step for 2 min at 50°C and pre-denaturation for 2 min at 95°C followed by 40 cycles of the following: denaturation for 15 s at 95°C and annealing for 1 min at 60°C. Relative gene expression was normalized to β-actin expression using the $2^{-\Delta\Delta Ct}$ method. Amplification of specific transcripts was confirmed based on the melting curves between 60°C and 95°C following PCR. Primers have been listed in the Table 1.

Protein extraction from the plasma membrane and cytosol

After 7 days treatment of 3T3-L1 cells with or without γ-HCH, the protein of both plasma membrane and cytosol were extracted by modifying a previously described protocol.[27] Cells were homogenized in ice-cold buffer A, i.e., M-PER mammalian protein extraction reagent (Thermo Scientific, IL) containing 0.1% (v/v) NP-40 (FUJIFILM Wako Pure Chemical Corporation, Osaka, Japan), protease inhibitor cocktail (Nacalai Tesque, Kyoto, Japan), and phosphatase inhibitor cocktail (Nacalai Tesque, Kyoto, Japan) by passing ten times through a 5/8-inch 27-gauge needle attached to syringe at 4°C. The homogenate was centrifuged at 1,000×g for 10 min at 4°C and the supernatant was collected and comprised the cytosolic fraction 1. The obtained precipitate was resuspended in NP-40-free buffer A and incubated on ice for 10 min with gentle mixing. Subsequently, the resuspended participates was centrifuged at 1,000×g for 10 min at 4°C and the supernatant was collected as cytosolic fraction 2. This precipitate was resuspended in buffer A containing 1.0% (v/v) NP-40 and incubated on ice for overnight with gentle mixing followed by centrifugation at 16,000×g for 30 min at 4°C. The supernatant was collected as the plasma membrane fraction. In this fraction, we confirmed that expression of ATPase protein, a marker of plasma membrane fraction, by immunoblotting. Finally, cytosolic fractions 1 and 2 were centrifuged at 16,000×g for 30 min at 4°C. The supernatants were collected as the final cytosolic fractions. All samples were stored at -80°C until further use.

Immunoblotting

The protein samples, which were described as above, were mixed with Laemmli's sample buffer and incubated in a heat block at 100°C for 3 min (cytosol fraction) and 37°C for 10 min (plasma membrane fraction). Cooled samples at room temperature were loaded onto a 9%–12% sodium dodecyl sulfate-polyacrylamide gel. After electrophoresis, the proteins were transferred onto a polyvinylidene fluoride (PVDF) membrane (Millipore Corporation, Billerica, MA). The PVDF membrane was first incubated for 5 min in Bullet Blocking One (Nacalai Tesque, Kyoto, Japan) at room temperature. After blocking, the PVDF membrane was incubated overnight with specific primary antibodies in Tris-buffered saline supplemented with Tween 20 at 4°C. We used the following primary antibodies at a 1:1,000 dilution: β-actin, ATPase (Abcam, Cambridge, UK), GLUT4 (Cell Signaling Technology, Inc., Danvers, MA), JNK, JNK phosphorylated at tyrosine-183/185 (Cell Signaling Technology), IRS-1 (Abcam), IRS-1 phosphorylated at serine-307 (Ser307) (Merck KGaA, Darmstadt, Germany), AKT-2, AKT-2 phosphorylated at serine-474 (Ser474), AS160, AS160 phosphorylated at serine-588 (Ser588) (Abcam). After washing, the membranes were incubated for 60 min with anti-rabbit or anti-mouse immunoglobulin G (1:2,000 or 5,000 dilution) antibodies

conjugated with horseradish peroxidase (DakoCytomation, Glostrup, Denmark) and TidyBlot western blot detection reagent:HRP (Bio-Rad Laboratories Inc., CA). The membranes were washed and immunoreactive bands were detected using Chemi-Lumi One Super (Nacalai Tesque, Kyoto, Japan) with the ChemiDoc imaging system (Bio-Rad Laboratories Inc., CA).

Enzyme-Linked Immuno Sorbent Assay of TNF-α

The protein levels of tumor necrosis factor-alpha (TNF-α) in the medium and cell lysate, were determined by commercially available kit in accordance with the manufacturer's instructions (R and D systems, MN).

Statistical analysis

Parametric data were represented as mean ± standard deviation. The mean values were compared by the Dunnett's test and Student's t-test. Non-parametric data was shown with boxplot. The values were compared by Mann-Whitney U test. $P < 0.05$ was considered statistically significant.

Results

As shown in Fig. 1A, cell viabilities were significantly reduced at 1,000 μM of γ-HCH compared with that in non-treated control cells (0 μM). No significant changes were observed at 25μM, 50 μM and 100 μM of γ-HCH. In 100 μM of γ-HCH, however, the cell viability had large variation compared with 50 μM of γ-HCH. We determined, therefore, 50 μM of γ-HCH as a sub-toxic dose of γ-HCH in this study. Under these conditions, γ-HCH significantly reduced insulin-stimulated glucose uptake as compared to that in control cells (Fig. 1B).

As shown in Fig. 2A, GLUT4 mRNA levels were significantly higher in γ-HCH-treated cells than that in control cells. The protein levels of GLUT4 were significantly increased and decreased in the cytosolic (Fig. 2B) and plasma membrane fractions (Fig 2C), respectively of γ-HCH-treated cells as compared to the levels in control cells. Intracellular ROS production was enhanced in γ-HCH-treated cells as compared to that in control cells (Fig. 2D). The exposure to γ-HCH enhanced the levels of ROS markers, such as cytochrome P450 1b1 (Fig. 3A), haptoglobin (Fig. 3B), ceruloplasmin (Fig. 3C), and xanthine dehydrogenase (Fig. 3D), as compared to those in the control cells. The levels of NADPH oxidase-4 (Nox-4) mRNA (Fig. 3E) and nuclear factor erythroid 2-related factor 2 (Nrf2) (Fig. 3F) were also significantly augmented in γ-HCH-treated cells.

Treatment with γ-HCH enhanced intracellular ROS levels and phosphorylation of JNK (Fig. 4A). Under this condition, γ-HCH also enhanced phosphorylation of IRS-1 at Ser307, a target of JNK (Fig. 4B). The phosphorylation of AKT2 was suppressed upon treatment with γ-HCH (Fig. 4C). Phosphorylation of AS160 was also downregulated by γ-HCH (Fig. 4D).

In the incubation medium, there were no change in the protein levels of TNF-α with or without g-HCH (Fig. 5A), while significant decrease was observed at the levels of both TNF-α mRNA (Fig. 5B) and protein (Fig. 5C) in the lysate of the cells exposed to γ-HCH compared to non-treated control cells.

Discussion

We firstly confirmed sub-toxic dose of γ-HCH in mature 3T3-L1 adipocytes as 50 μM, and applied the concentration for whole experiments in this study. Thereby the results of this study are thought to be occurred under the normal situation without cell damage.

This study demonstrated that the addition of γ-HCH significantly reduced glucose uptake by fully differentiated mature 3T3-L1 adipocytes via the increased phosphorylation of IRS-1 at Ser307 following JNK activation that impaired insulin-related signal transduction and resulted in insulin resistance. This was supported by the following experimental data. GLUT4 protein levels in the plasma membrane decreased in γ-HCH-treated cells as compared with that in untreated control cells, although the mRNA and protein levels of GLUT4 in the cytosol fraction were higher in γ-HCH-treated cells

than those in the untreated control cells. In addition, γ-HCH augmented intracellular ROS generation with elevation in the mRNA levels of ROS markers as compared to those in the control cells. Moreover, γ-HCH hindered the phosphorylation of AKT2 and AS160, downstream molecules of phosphorylated IRS-1 at Ser307, suggesting a negative role of γ-HCH on glucose uptake via the inhibition of GLUT4 translocation from the cytosol to the plasma membrane, thereby causing insulin resistance in mature 3T3-L1 adipocytes.

γ-HCH enhanced intracellular ROS production in differentiated 3T3-L1 mature adipocytes; this is in accordance with the enhanced generation of ROS in other cells, such as renal distal tubule cells,[28] dopaminergic neurons,[29] and Ehrlich ascites tumor cells.[30] NADPH oxidase-1 (Nox-1), a key enzyme involved in the production of cellular ROS, has a prominent role in γ-HCH-induced ROS generation in dopaminergic neurons.[31] Interestingly, Nox-4, a member of the NADPH oxidase family of proteins, is only expressed in 3T3-L1 adipocytes.[32] A dramatic increase in the ROS content of adipocytes has shown to be related with elevation of Nox-4 mRNA and protein.[20] Moreover, Nrf2 mRNA levels are associated with the increased ROS generation in rat white adipocytes.[21] Consequently, the γ-HCH-induced increase in ROS generation might be regulated by Nox-4 along with elevated levels of Nrf2 mRNA in 3T3-L1 adipocytes. This is in accordance with the findings of this study: γ-HCH induced the overexpression of Nox-4 and Nrf2 mRNAs.

JNK activation is enhanced by oxidative stress in 3T3-L1 adipose cells[33,34] and ROS-mediated activation of JNK promotes insulin resistance in adipose cells.[35,36] Previous studies have demonstrated that the mechanism underlying JNK-mediated insulin resistance is closely associated with the phosphorylation of Ser307 in IRS-1.[25,37] The knockdown of JNK rescues insulin resistance in 3T3-L1 adipocytes[38] and the inactivation of JNK attenuates Ser307 phosphorylation of IRS-1 and confers insulin resistance in 3T3-L1 adipocytes.[39] Our data also demonstrated that the γ-HCH-stimulated phosphorylation of Ser307 in IRS-1 inactivated AKT2 and AS160, resulting in the reduced translocation of GLUT4 from the cytosol to the plasma membrane. Therefore, γ-HCH-induced phosphorylation of Ser307 in IRS-1 might play a critical role in the attenuation of insulin-stimulated glucose uptake, which is mediated by the translocation of GLUT4 protein. These results indicate that ROS-mediated activation of JNK upon treatment with γ-HCH inhibits the insulin-stimulated translocation of GLUT4 protein via an increase in the phosphorylation of IRS-1 at Ser307, thereby reducing insulin-stimulated glucose uptake in 3T3-L1 adipocytes.

On the other hand, it has been widely accepted that TNF-α also attenuates insulin-induced glucose uptake via impaired insulin signaling.[40-42] One of the mechanisms underlying TNF-α-induced insulin resistance has shown to involve the phosphorylation of Ser307 in IRS-1.[43,44] Therefore, it was hypothesized that γ-HCH increases the secretion of TNF-α from adipocytes, thereby stimulating the phosphorylation of Ser307 in IRS-1 in adipose cells via autocrine and paracrine signaling. However, γ-HCH had no effect on the secretion of TNF-α from mature 3T3-L1 adipocytes into the culture medium, although the levels of both TNF-α mRNA and protein was significantly reduced in γ-HCH-treated cells as compared to those in control cells. Thus, the ability of γ-HCH at phosphorylating Ser307 in IRS-1 through enhanced JNK activation via increase in ROS generation might be independent on TNF-α-induced phosphorylation event of IRS-1. These results suggest that γ-HCH-induced reduction of insulin-stimulated glucose uptake is independent of secreted TNF-α from cell themselves.

In conclusion, γ-HCH exhibited inhibitory effects on the insulin-stimulated uptake of glucose by mature 3T3-L1 adipocytes via ROS generation, JNK-induced phosphorylation of Ser307 of IRS-1, impaired translocation of GLUT4 protein from the cytosol to the plasma membrane, and inhibition of insulin signaling. Therefore, the findings of this study indicate that sub-toxic exposure to γ-HCH causes insulin resistance in mammalian mature adipocytes, and that removal of γ-HCH from the environment prevents γ-HCH-induced diabetes and other metabolic disorders.

Conclusion

The present study demonstrated that γ-HCH attenuated glucose uptake in fully differentiated 3T3-L1 adipocytes through enhanced intracellular ROS and activated JNK. Under this condition, JNK-

stimulated phosphorylation of Ser307 in IRS-1 impaired the activity of downstream molecules, thereby inhibiting the translocation of GLUT4 protein on the plasma membrane.

Abbreviations

γ-HCH: gamma-hexachlorocyclohexane; ROS: reactive oxygen species; GLUT4: glucose transporter 4; JNK: c-Jun N-terminal kinase; IRS-1: insulin receptor substrate-1; AS160: Akt Substrate of 160 kDa; TNF-α: tumor necrosis factor alpha

Acknowledgements

Funding: This study was supported in part by Asahikawa Medical University Fund.

Competing interests

The authors declare that they have no competing interests.

References

1) Xu Y, Wang L, He J, et al. Prevalence and control of diabetes in Chinese adults. JAMA 310: 948-959, 2013
2) Misra A, Gopalan H, Jayawardena R, et al. Diabetes in developing countries. J Diabetes 11: 522-539, 2019
3) Lee DH, Steffes MW, Sjödin A, et al. Low dose of some persistent organic pollutants predicts type 2 diabetes: a nested case-control study. Environ Health Perspect 118: 1235-1242, 2010
4) Wu H, Bertrand KA, Choi AL, et al. Persistent organic pollutants and type 2 diabetes: a prospective analysis in the nurses' health study and meta-analysis. Environ Health Perspect 121: 153-161, 2013
5) Lee DH, Lee IK, Jin SH, et al. Association between serum concentrations of persistent organic pollutants and insulin resistance among nondiabetic adults: results from the National Health and Nutrition Examination survey 1999-2002. Diabetes Care 30: 622-628, 2007
6) Turyk M, Anderson HA, Knobeloch L, et al. Prevalence of diabetes and body burdens of polychlorinated biphenyls, polybrominated diphenyl ethers, and p,p'-diphenyldichloroethene in Great Lakes sport fish consumers. Chemosphere 75: 674-679, 2009
7) Wacławek S, Silvestri D, Hrabák P, et al. Chemical oxidation and reduction of hexachlorocyclohexanes: a review. Water Res 162: 302-319, 2019
8) Saez JM, Benimeli CS, Amoroso MJ. Lindane removal by pure and mixed cultures of immobilized actinobacteria. Chemosphere 89: 982-987, 2012
9) Lee DH, Lee IK, Song K, et al. A strong dose-response relation between serum concentrations of persistent organic pollutants and diabetes: results from the National Health and Examination survey 1999-2002. Diabetes Care 29: 1638-1644, 2006
10) Daglioglu N, Gulmen MK, Akcan R, et al. Determination of organochlorine pesticides residues in human adipose tissue, data from Cukurova, Turkey. Bull Environ Contam Toxicol 85: 97-102, 2010
11) Mustieles V, Fernández MF, Martin-Olmedo P, et al. Human adipose tissue levels of persistent organic pollutants and metabolic syndrome components: combining a cross-sectional with a 10-year longitudinal study using a multi-pollutant approach. Environ Int 104: 48-57, 2017
12) Singh VK, Sarkar SK, Saxena A, et al. Sub-toxic exposure to lindane activates redox sensitive kinases and impairs insulin signaling in muscle cell culture: the possible mechanism of lindane-induced insulin resistance. Toxicol In Vitro 54: 98-104, 2019
13) Satoh T. Molecular Mechanisms for the regulation of insulin-stimulated glucose uptake by small guanosine triphosphatases in skeletal muscle and adipocytes. Int J Mol Sci 15: 18677-18692, 2014
14) Sayem ASM, Arya A, Karimian H, et al. Action of phytochemicals on insulin signaling pathways accelerating glucose transporter (GLUT4) protein translocation. Molecules 23: 258, 2018
15) Bryant NJ, Gould GW. Insulin stimulated GLUT4 translocation – size is not everything!. Curr

Opin Cell Biol 65: 28-34, 2020
16) Ma M, Quan Y, Li Y, et al. Bidirectional modulation of insulin action by reactive oxygen species in 3T3-L1 adipocytes. Mol Med Rep 18: 807-814, 2018
17) Srivastava A, Shivanandappa T. Stereospecificity in the cytotoxic action of hexachlorocyclohexane isomers. Chem Biol Interact 183: 34-39,2010
18) Michałowicz J, Mokra K, Rosiak K, et al. Chlorobenzenes, lindane and dieldrin induce apoptotic alterations in human peripheral blood lymphocytes (in vitro study). Environ Toxicol Pharmacol 36: 979-988, 2013
19) Houstis N, Rosen ED, Lander ES. Reactive oxygen species have a causal role in multiple forms of insulin resistance. Nature 440: 944-948, 2006
20) Schröder K, Wandzioch K, Helmcke I, et al. Nox4 acts as a switch between differentiation and proliferation in preadipocytes. Arterioscler Thromb Vasc Biol 29:239-245, 2009
21) Illesca PG, Álvarez SM, Selenscig DA, et al. Dietary soy protein improves adipose tissue dysfunction by modulating parameters related with oxidative stress in dyslipidemic insulin-resistant rats. Biomed Pharmacother 88:1008-1015, 2017
22) Iordanov MS, Magun BE. Different mechanisms of c-Jun NH2-terminal Kinase-1 (JNK1) activation by ultraviolet-B radiation and by oxidative stressors. J Biol Chem 274: 25801-25806, 1999
23) Lacombe VA. Expression and regulation of facilitative glucose transporters in equine insulin-sensitive tissue: from physiology to pathology. ISRN Vet Sci 409547, 2014
24) Huang X, Liu G, Guo J, Su Z. The PI3K/AKT pathway in obesity and type 2 diabetes. Int J Biol Sci 14: 1483-1496, 2018
25) Aguirre V, Uchida T, Yenush L, et al. The c-Jun NH(2)-terminal kinase promotes insulin resistance during association with insulin receptor substrate-1 and phosphorylation of Ser(307). J Biol Chem 275: 9047-9054, 2000
26) Tanti JF, Jager J. Cellular mechanisms of insulin resistance: role of stress-regulated serine kinases and insulin receptor substrates (IRS) serine phosphorylation. Curr Opin Pharmacol 9: 753-762, 2009
27) Nishiumi S, Ashida H. Rapid preparation of a plasma membrane fraction from adipocytes and muscle cells: application to detection of translocated glucose transporter 4 on the plasma membrane. Biosci Biotechnol Biochem 71: 2343-2346, 2007
28) Piskac-Collier AL, Smith MA. Lindane-induced generation of reactive oxygen species and depletion of glutathione do not result in necrosis in renal distal tubule cells. J Toxicol Environ Health A 72: 1160-1167, 2009
29) Sharma H, Zhang P, Barber DS, et al. Organochlorine pesticides dieldrin and lindane induce cooperative toxicity in dopaminergic neurons: role of oxidative stress. Neurotoxicology 31: 215-22, 2010
30) Srivastava A, Shivanandappa T. Causal relationship between hexachlorocyclohexane cytotoxicity, oxidative stress and Na+, K +-ATPase in Ehrlich ascites tumor cells. Mol Cell Biochem 286: 87-93, 2006
31) Sharma H, Hirko AC, King MA, et al. Role of NADPH oxidase in cooperative reactive oxygen species generation in dopaminergic neurons induced by combined treatment with dieldrin and lindane. Toxicol Lett 299: 47-55, 2018
32) Han CY, Umemoto T, Omer M, et al. NADPH oxidase-derived reactive oxygen species increases expression of monocyte chemotactic factor genes in cultured adipocytes. J Biol Chem 287: 10379-10393, 2012
33) Ge X, Yu Q, Qi W, Shi X, Zhai Q. Chronic insulin treatment causes insulin resistance in 3T3-L1 adipocytes through oxidative stress. Free Radic Res 42: 582-591, 2008
34) Tatsumi F, Kaneto H, Hashiramoto M, et al. Anti-hypertensive azelnidipine preserves insulin signaling and glucose uptake against oxidative stress in 3T3-L1 adipocytes. Endocr J 62: 741-747, 2015
35) Ge X, Liu Z, Qi W, et al. Chromium (VI) induces insulin resistance in 3T3-L1 adipocytes through elevated reactive oxygen species generation. Free Radic Res 42: 554-563, 2008
36) Davis JE, Gabler NK, Walker-Daniels J, et al. The c-Jun N-terminal kinase mediates the induction

of oxidative stress and insulin resistance by palmitate and toll-like receptor 2 and 4 ligands in 3T3-L1 adipocytes. Horm Metab Res 41: 523-530, 2009
37) Aguirre V, Werner ED, Giraud J, et al. Phosphorylation of Ser307 in insulin receptor substrate-1 blocks interactions with the insulin receptor and inhibits insulin action. J Biol Chem 277: 1531-1537, 2002
38) Kim T, Wayne Leitner J, Adochio R, Draznin B. Knockdown of JNK rescues 3T3–L1 adipocytes from insulin resistance induced by mitochondrial dysfunction. Biochem Biophys Res Commun 378: 772-776, 2009
39) Ye L, Liang S, Guo C, et al. Inhibition of M1 macrophage activation in adipose tissue by berberine improves insulin resistance. Life Sci 166: 82-91, 2016
40) Hotamisligil GS, Shargill NS, Spiegelman BM. Adipose expression of tumor necrosis factor-alpha: direct role in obesity-linked insulin resistance. Science 259: 87-91, 1993
41) Feinstein R, Kanety H, Papa MZ, Lunenfeld B, Karasik A. Tumor necrosis factor-alpha suppresses insulin-induced tyrosine phosphorylation of insulin receptor and its substrates. J Biol Chem 268: 26055-26058, 1993
42) Hotamisligil GS, Spiegelman BM. Spiegelman, Tumor necrosis factor alpha: a key component of the obesity-diabetes link. Diabetes 43: 1271-1278, 1994
43) Rui L, Aguirre V, Kim JK, Shulman GI, Lee A, Corbould A, et al. Insulin/IGF-1 and TNF-alpha stimulate phosphorylation of IRS-1 at inhibitory Ser307 via distinct pathways. J Clin Invest 107: 181-189, 2001
44) Gao Z, Zuberi A, Quon MJ, et al. Aspirin inhibits serine phosphorylation of insulin receptor substrate 1 in tumor necrosis factor-treated cells through targeting multiple serine kinases. J Biol Chem 278: 24944-24950, 2003

Figure legends

Figure 1. Effect of γ-HCH on cell viability and glucose uptake in mature 3T3-L1 adipocytes
(A) The cell viability. Bars and vertical lines indicate mean ± standard deviation (SD). (B) Glucose uptake. *P<0.05.

Figure 2. Effect of γ-HCH on the mRNA and protein levels of GLUT4 and ROS generation in mature 3T3-L1 adipocytes
(A) The mRNA and (B) protein levels of GLUT4 in the cytosol fraction, (C) protein levels of GLUT4 in the plasma membrane, (D) intracellular reactive oxygen species (ROS) levels. Results were representative of three independent experiment (n = 5 for each group). Bars and vertical lines indicate mean ± SD. *P<0.05.

Figure 3. Effect of γ-HCH on the mRNA levels of ROS markers
(A) Cytochrome P450 1b1, (B) haptoglobin, (C) ceruloplasmin 350, (D) xanthine dehydrogenase. (E) NADPH oxidase-4 (Nox-4), and(F) nuclear factor erythroid 2-related factor 2 (Nrf2). Bars and vertical lines indicate mean ± SD. *P<0.05.

Figure 4. Effect of γ-HCH on the expression and phosphorylation of JNK, IRS-1, AKT2, and AS160 in mature 3T3-L1 adipocytes
Phosphorylation of (A) JNK and (B) IRS-1, (C) AKT2 and (D) AS160. Results were representative of three independent experiment (n = 5 for each group). Bars and vertical lines indicate mean ± SD. *P<0.05.

Figure5. Effect of γ-HCH on secretion of TNF-α into the cell culture medium and TNF-α mRNA and its protein in the lysate of mature 3T3-L1 adipocytes.
(A) secretion levels of TNF-α into the cell culture medium, (B) TNF-α mRNA and (C) its protein in the lysate. Bars and vertical lines indicate mean ± SD. * P < 0.05 vs control values.

Figure 6. The schematic model of the current study
Intracellular ROS generation is increased by treatment of γ-HCH, in turn, JNK is activated via its phosphorylation. Activated-JNK provokes phosphorylation of IRS-1 at Ser307. Consequently, translocation of GLUT4 from the cytosol to the plasma membrane is impaired, thereby attenuating the glucose uptake into mature 3T3-L1 adipocytes.

Table 1. Primer sequences for RT-qPCR

A

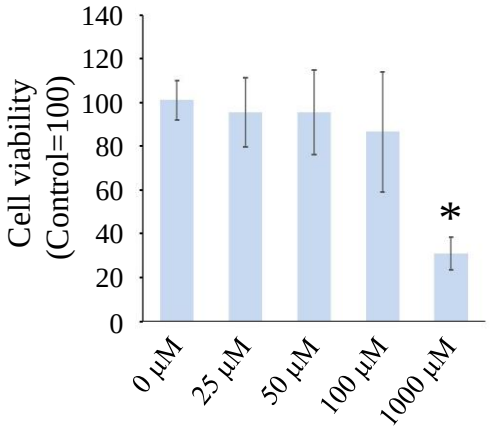
Cell viability
(Control=100)
140
120
100
80
60
40
20
0
*
0 μM
25 μM
50 μM
100 μM
1000 μM

B

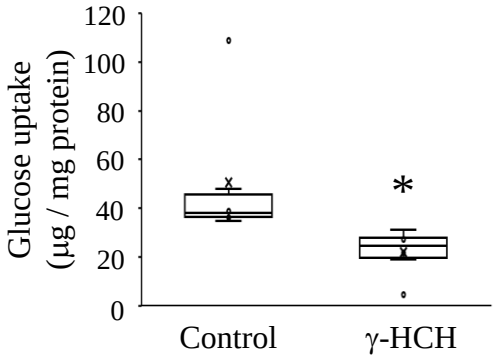
Glucose uptake
(μg / mg protein)
120
100
80
60
40
20
0
*
Control
γ-HCH

Figure 1

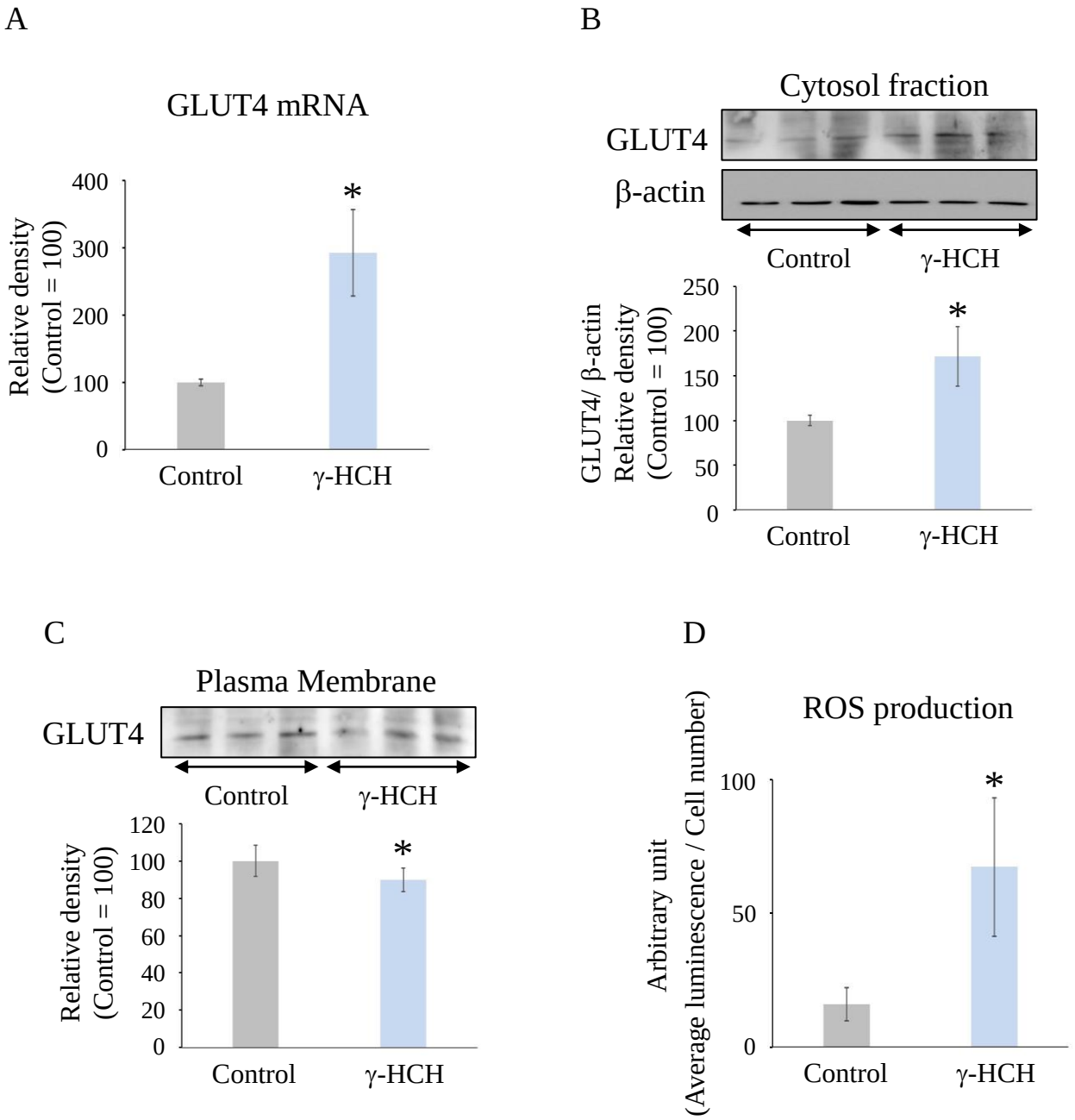
A
GLUT4 mRNA
Relative density
(Control = 100)
400
300
200
100
0
*
Control
γ-HCH
B
Cytosol fraction
GLUT4
β-actin
Control
γ-HCH
GLUT4/ β-actin
Relative density
(Control = 100)
250
200
150
100
50
0
*
Control
γ-HCH
C
Plasma Membrane
GLUT4
Control
γ-HCH
Relative density
(Control = 100)
120
100
80
60
40
20
0
*
Control
γ-HCH
D
ROS production
Arbitrary unit
(Average luminescence / Cell number)
100
50
0
*
Control
γ-HCH

Figure 2

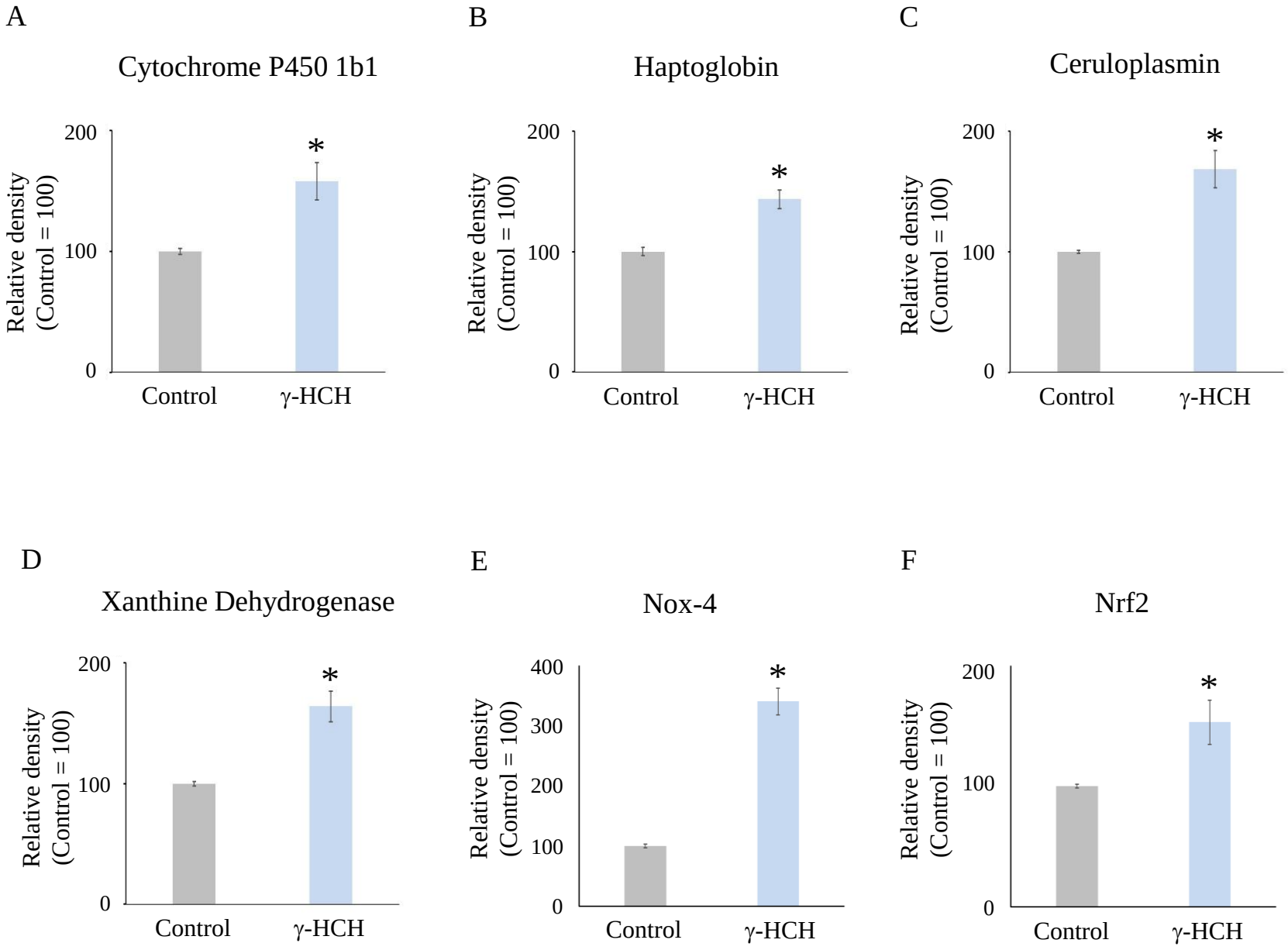
A
Cytochrome P450 1b1
Relative density (Control = 100)
200
100
0
*
Control
γ-HCH
B
Haptoglobin
Relative density (Control = 100)
200
100
0
*
Control
γ-HCH
C
Ceruloplasmin
Relative density (Control = 100)
200
100
0
*
Control
γ-HCH
D
Xanthine Dehydrogenase
Relative density (Control = 100)
200
100
0
*
Control
γ-HCH
E
Nox-4
Relative density (Control = 100)
400
300
200
100
0
*
Control
γ-HCH
F
Nrf2
Relative density (Control = 100)
200
100
0
*
Control
γ-HCH

Figure 3

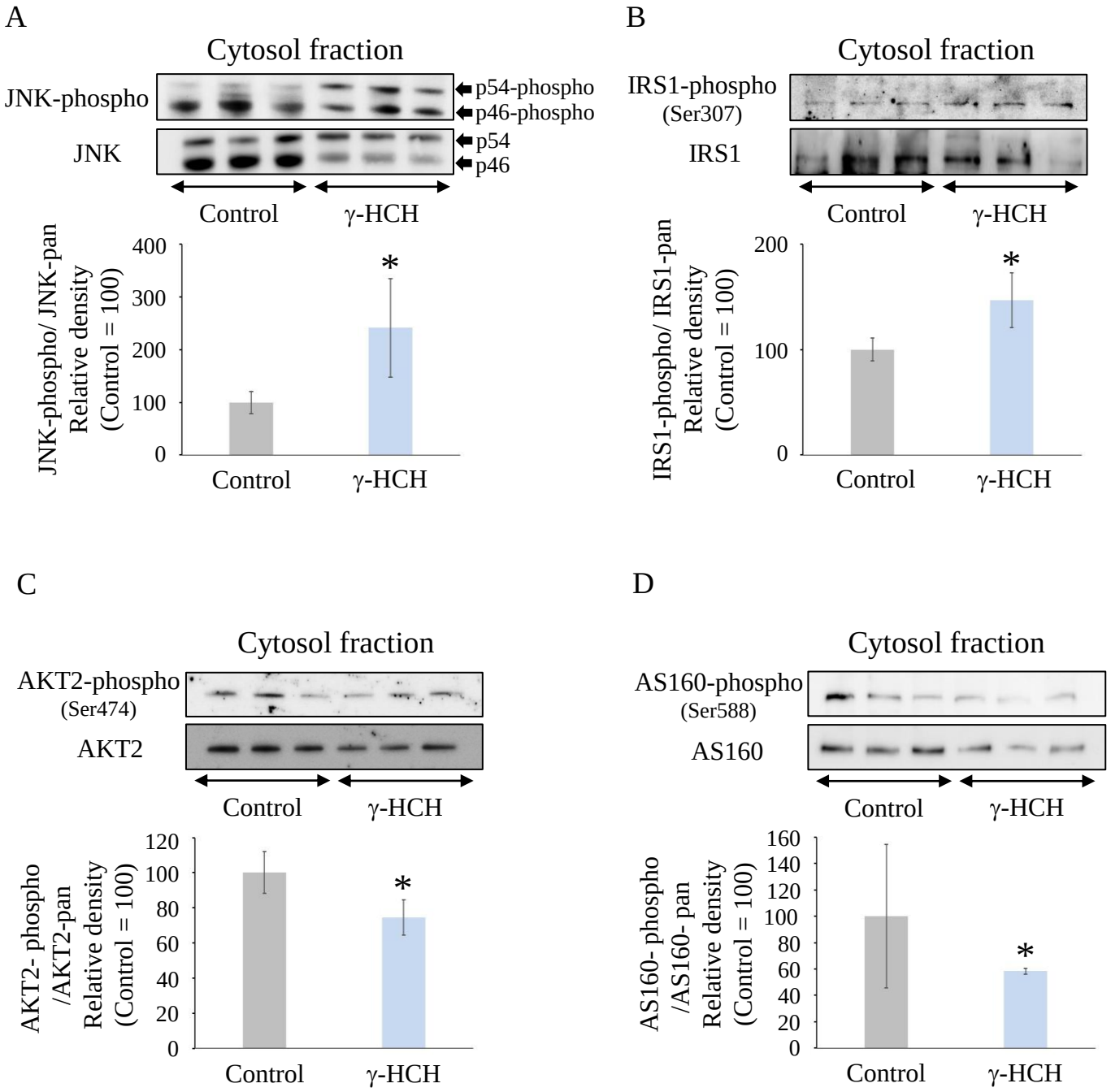
A
Cytosol fraction
JNK-phospho
p54-phospho
p46-phospho
JNK
p54
p46
Control
γ-HCH
JNK-phospho/ JNK-pan
Relative density
(Control = 100)
400
300
200
100
0
*
Control
γ-HCH
B
Cytosol fraction
IRS1-phospho
(Ser307)
IRS1
Control
γ-HCH
IRS1-phospho/ IRS1-pan
Relative density
(Control = 100)
200
100
0
*
Control
γ-HCH
C
Cytosol fraction
AKT2-phospho
(Ser474)
AKT2
Control
γ-HCH
AKT2- phospho
/AKT2-pan
Relative density
(Control = 100)
120
100
80
60
40
20
0
*
Control
γ-HCH
D
Cytosol fraction
AS160-phospho
(Ser588)
AS160
Control
γ-HCH
AS160- phospho
/AS160- pan
Relative density
(Control = 100)
160
140
120
100
80
60
40
20
0
*
Control
γ-HCH

Figure 4

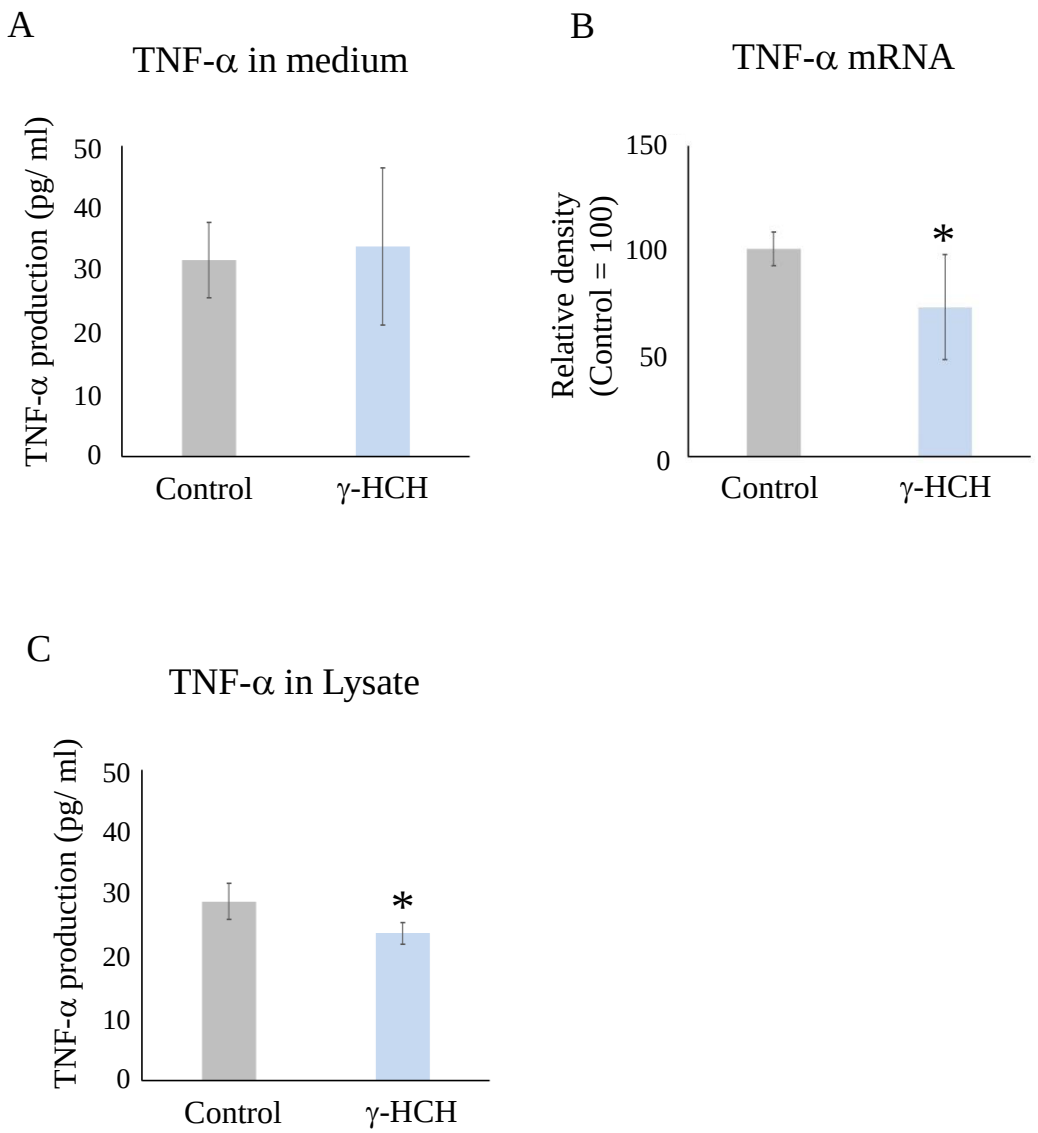
A
TNF-α in medium
TNF-α production (pg/ ml)
50
40
30
20
10
0
Control
γ-HCH
B
TNF-α mRNA
Relative density
(Control = 100)
150
100
50
0
*
Control
γ-HCH
C
TNF-α in Lysate
TNF-α production (pg/ ml)
50
40
30
20
10
0
*
Control
γ-HCH

Figure 5

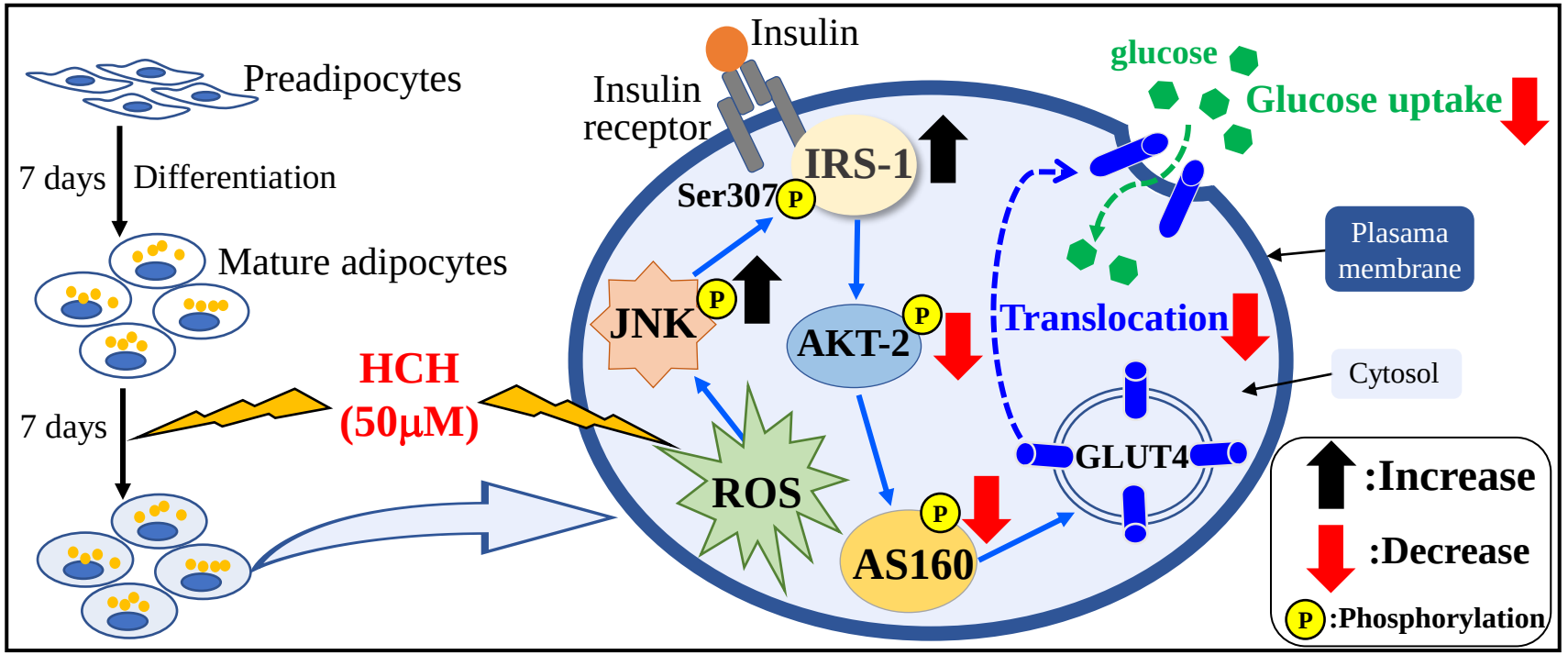
Preadipocytes
7 days
Differentiation
Mature adipocytes
7 days
HCH
(50μM)
Insulin
Insulin
receptor
IRS-1
Ser307
P
JNK
AKT-2
ROS
AS160
glucose
Glucose uptake
Plasama
membrane
Translocation
Cytosol
GLUT4
:Increase
:Decrease
:Phosphorylation

Figure 6

Table 1 Primer sequences for RT-qPCR

Primer name	Primer Length (mer)	Amplaic on Size (bp)	Sequence
β-actin	21	237 bp	Sense: 5'-TCGTACCACAGGCATTGTGAT-3'
	20		Antisense: 5'-TGCTCGAAGTCTAGAGCAAC-3'
GLUT4	20	99 bp	Sense: 5'- GCCTGCCCGAAAGAGTCTAA-3'
	20		Antisense: 5'-CGCTCTCTCTCCAACTTCCG-3'
Cytochrome P450,1b1	22	234 bp	Sense: 5'-TATTACGGACATCTTCGGAGCC-3'
	20		Antisense: 5'-TGTGGAATGGTGACAGGCAA-3'
Haptoglobin	20	196 bp	Sense: 5'-GTGGAGCACTTGGTTCGCTA-3'
	21		Antisense: 5'-CCATAGAGCCACCGATGATGC-3'
Ceruloplasmin	20	226 bp	Sense: 5'-CCTGGAGTCTGGATGCTCAG-3'
	24		Antisense:5'-CTGAATCACTTCCAGAGGCTGTTA-3'
Xanthine Dehydrogenase	20	120 bp	Sense:5'-GGATGCTAATCGCAGAATAC-3'
	20		Antisense: 5'-GCTTCTGGTTGAAGTGAGTC-3'
Nox-4	20	196 bp	Sense: 5'-GTGTCTGCATGGTGGTGGTA-3'
	20		Antisense: 5'-AGACTAATGCAGCCAGGAGG-3'
Nrf2	20	178 bp	Sense: 5'-AGCTGGCTGATACTACCGCT-3'
	20		Antisense: 5'-CTGGCACATCAGTGGAGAGG-3'

Abbreviations: GLUT4: glucose transporter 4; Nox-4: NADPH oxidase-4; Nrf2: Nuclear factor erythroid 2-related factor 2